Differential Interaction of Equinatoxin II with Model Membranes in Response to Lipid Composition

José M. M. Caaveiro, Izaskun Echabe, Ion Gutiérrez-Aguirre, José L. Nieva, José L. R. Arrondo, and Juan M. González-Mañas

Unidad de Biofísica (CSIC-UPV/EHU) and Departamento de Bioquímica y Biología Molecular, Universidad del País Vasco, Apartado 644, 48080 Bilbao, Spain

ABSTRACT Equinatoxin II is a 179-amino-acid pore-forming protein isolated from the venom of the sea anemone *Actinia equina*. Large unilamellar vesicles and lipid monolayers of different lipid compositions have been used to study its interaction with membranes. The critical pressure for insertion is the same in monolayers made of phosphatidylcholine or sphingomyelin (~26 mN m^{-1}) and explains why the permeabilization of large unilamellar vesicles by equinatoxin II with these lipid compositions is null or moderate. In phosphatidylcholine-sphingomyelin (1:1) monolayers, the critical pressure is higher (~33 mN m^{-1}), thus permitting the insertion of equinatoxin II in large unilamellar vesicles, a process that is accompanied by major conformational changes. In the presence of vesicles made of phosphatidylcholine, a fraction of the protein molecules remains associated with the membranes. This interaction is fully reversible, does not involve major conformational changes, and is governed by the high affinity for membrane interfaces of the protein region comprising amino acids 101–120. We conclude that although the presence of sphingomyelin within the membrane creates conditions for irreversible insertion and pore formation, this lipid is not essential for the initial partitioning event, and its role as a specific receptor for the toxin is not so clear-cut.

INTRODUCTION

Equinatoxin II (EqT-II) is the most abundant hemolytic toxin isolated from the sea anemone *Actinia equina*. It is a 179-amino-acid residue protein with a molecular mass of 19.8 kDa and an isoelectric point of 10.5 (Maček and Lebez, 1988). Numerous cytolytic and cytotoxic effects on mammalian cells have been described so far, e.g., in red blood cells (Maček and Lebez, 1981), platelets (Teng et al., 1988), tumor cell lines (Giraldi et al., 1976), fibroblasts (Batista et al., 1987), bovine lactotrophs (Zorec et al., 1990), and cardiac cells (Bunc et al., 1999). All these effects are due, at least in part, to the ability of EqT-II to bind to the cell membrane and form pores with an estimated functional radius of 1.1 nm (Zorec et al., 1990; Belmonte et al., 1993; Maček et al., 1994).

The interaction of EqT-II with model membranes results in the formation of cation-selective channels in planar lipid bilayers (Zorec et al., 1990; Belmonte et al., 1993; Maček et al., 1994) and the permeabilization of small and large unilamellar vesicles (Belmonte et al., 1993; Maček et al., 1994, 1995, 1997). This interaction is associated with changes in the secondary and tertiary structure of the protein (Maček et al., 1995; Belmonte et al., 1994; Poklar et al., 1999), and it has been suggested that the transition from the water-soluble to the membrane-bound state of the protein takes place through a molten-globule intermediate (Poklar et al., 1997). The insertion of EqT-II in model membranes largely depends on the presence of sphingomyelin within the bilayer (Belmonte et al., 1993; Maček et al., 1995). This feature is common to other cytolysins from sea anemones (Tejuca et al., 1996; De los Ríos et al., 1998), and some authors have suggested that sphingomyelin might be a specific receptor for cytolysins (Bernheimer and Avigad, 1976; Turk and Maček, 1986).

In this work we have used different model membranes and biophysical techniques to further explore the interaction of EqT-II with the lipid bilayer, paying special attention to the differential effects observed in membranes with different compositions.

MATERIALS AND METHODS

Materials

Egg phosphatidylcholine (PC) and egg phosphatidylethanolamine (PE) were grade I from Lipid Products (South Nutfield, UK). Dipalmitoylphosphatidylcholine (DPPC) and bovine brain sphingomyelin (SM) were from Avanti Polar Lipids (Alabaster, AL). Cholesterol (Cho) and Triton X-100 were from Sigma (St. Louis, MO). 8-Aminonaphthalene-1,3,6-trisulfonic acid (ANTS) and *p*-xylene-*bis*-pyridiniumbromide (DPX) were from Molecular Probes (Eugene, OR). Poly (ethylene-glycol 10,000) (PEG-10,000) was from Atlas (Sao Paulo, Brazil). Horse erythrocytes were from Biomedics (Alcobendas, Spain).

Purification of the protein

Equinatoxin II (EqT II) was purified from the liquid exuded by freshly collected *Actinia equina* specimens in the Cantabrian sea. We followed the purification protocol described by Maček and Lebez (1988). The purified protein was concentrated to approximately 10 mg/ml with an Amicon 8050 (Danvers, MA) ultrafiltration unit equipped with a regenerated nitrocellulose filter (Millipore, Bedford, MA) with a molecular weight cutoff

Received for publication 8 May 2000 and in final form 7 December 2000.

Address reprint requests to Dr. Juan M. González-Mañas, Departamento de Bioquímica y Biología Molecular, Universidad del País Vasco, Apartado 644, 48080 Bilbao, Spain. Tel.: 3494-601-5379; Fax: 3494-464-8500; E-mail: gbpgomaj@lg.ehu.es.

0006-3495/01/03/1343/11 $2.00

(MWCO) of 10 kDa. Aliquots of the concentrated protein were stored at −24°C, and once thawed they were not refrozen. Protein concentration was estimated spectrophotometrically using a molar extinction coefficient at 280 nm of 3.61×10^4 M^{-1} cm^{-1} (Norton et al., 1992).

Hemolytic activity

The equinatoxin II-induced hemolysis of horse erythrocytes was determined as a decrease in the turbidity of a cell suspension using a Uvikon 943 spectrophotometer (Kontron Instruments, Milan, Italy) with the wavelength set at 720 nm. The hemolysis buffer was 10 mM HEPES, 145 mM NaCl, 2mM PEG-10,000, pH 7.5. The experiment was carried out at 25°C and under constant stirring. The maximum velocity of hemolysis was obtained from the region of the hemolytic curve showing maximum slope. The relationship between sample turbidity and erythrocyte concentration was determined using a Coulter counter apparatus from Coulter Electronics (Luton, UK) and obeys the following equation: $y = 2.24 \times 10^6x^2 + 4.79 \times 10^6x + 0.15 \times 10^6$, where y is the number of erythrocytes per milliliter and x is the turbidity at 720 nm.

Preparation of liposomes

The appropriate lipids were mixed in organic solvent and evaporated thoroughly. Multilamellar liposomes (MLVs) were prepared by hydration of the lipid film with buffer and intensive vortexing. Large unilamellar vesicles (LUVs) were prepared by the extrusion method (Mayer et al., 1986), using polycarbonate filters with a pore size of 0.1 μm (Nuclepore, Pleasanton, CA). Liposomes were routinely prepared in 10 mM HEPES, 200 mM NaCl, pH 7.5 buffer. For assays of vesicle leakage, the buffer contained in addition 25 mM ANTS and 90 mM DPX. Non-encapsulated fluorescent probes were separated from the vesicle suspension through a Sephadex G-75 gel filtration column (Pharmacia, Uppsala, Sweden). Solution osmolarities were measured using an Osmomat 030 instrument (Gonotec, Berlin, Germany). Phospholipid concentration was determined according to Bartlett (1959).

Assay for leakage of liposomal contents

The leakage of encapsulated solutes was assayed as described by Ellens et al. (1985), using ANTS and DPX. The probe-loaded liposomes (final lipid concentration = 0.1 mM) were treated with the appropriate amounts of protein in a fluorometer cuvette, at 25°C and under constant stirring. Changes in fluorescence intensity were recorded in a Perkin-Elmer MPF-66 spectrofluorometer (Beaconsfield, UK) with excitation and emission wavelengths set at 350 and 510 nm, respectively. An interference filter with a nominal cutoff value of 470 nm was placed in the emission light path to minimize the scattered-light contribution of the vesicles to the fluorescence signal. The percentage of leakage is calculated after all of the fluorescent probe is released by the addition of the nonionic detergent Triton X-100. The parameter $T_{1/2}$ represents the time needed to reach 50% of the final leakage.

Liposome aggregation assay

Kinetics of vesicle aggregation was routinely followed as an increase in light scattering at 90° in a Perkin-Elmer MPF-66 fluorometer with both monochromators set at 520 nm. Aggregation was also measured under apparent equilibrium conditions as an increase in the average particle size, measured by quasi-elastic light scattering (QELS) in a Zetasizer 4 photometer (Malvern, UK). For QELS measurements buffer solutions were previously filtered through 0.22-μm pore-size filters.

Binding experiments

Binding of EqT-II to LUVs was measured by a filtration method using Centrisart I units (Sartorius, Göttingen, Germany). The Centrisart I units contained a polysulfone membrane with an MWCO of 300 kDa, which allowed the physical separation of free toxin from toxin bound to the liposomes. Different amounts of protein were added to a fixed amount of vesicles. Samples were allowed to equilibrate for 2 h at 25°C and then applied to the Centrisart I units and centrifuged at 2000 × g. The concentration of free EqT-II was determined by measuring the absorbance at 280 nm of the liposome-free fraction. The amount of bound protein was calculated as the difference between total and unbound protein. Interaction of the water-soluble toxin with membranes is better described as a partition process between the liposomes and the aqueous phase (White et al., 1998; White and Wimley, 1999). The partition coefficient (K_X) is therefore defined as:

$$K_X = \frac{X_V}{X_A}, \tag{1}$$

where X_V is the molar fraction of the protein bound to the vesicles and X_A is the molar fraction of the protein in the aqueous phase. Once we have determined the partition coefficient it is possible to calculate the free energy of the transfer of the protein from the aqueous to the lipid phase:

$$\Delta G_X^0 = -RT \ln K_X, \tag{2}$$

where ΔG_x^0 is the free energy, R the gas constant, T the absolute temperature, and K_x the partition coefficient.

Infrared spectroscopy

The appropriate amount of protein was thawed and dried in a Savant evaporator (Farmingdale, NY). It was resuspended with the corresponding volume of buffer (either in aqueous or deuterated medium) to give a final protein concentration of 8 mg/ml. LUVs were prepared as described above, and when necessary, deuterated buffer was used. Vesicles and protein were mixed to give a lipid to protein ratio of 75:1 and incubated overnight at room temperature. The sample was placed in a thermostatted cell with CaF_2 windows. The optical path was 6 μm for samples in water and 50 μm for samples in D_2O. Spectra were recorded at 25°C in a Nicolet Magna 550 spectrophotometer equipped with a mercury-cadmium-tellurium (MCT) detector. Sample and reference spectra consisted of 1000 scans, with a nominal resolution of 2 cm^{-1}. For temperature studies, the sample was heated from 30°C to 80°C at 3°C intervals, and it was allowed to equilibrate for 8 min before each spectrum was recorded. Data treatment and band decomposition of the original amide I have been described previously (Cheín et al., 1999, and references therein).

Fluorescence spectroscopy

The intrinsic fluorescence spectra of EqT-II either alone or in the presence of vesicles were recorded in a Perkin-Elmer MPF-66 spectrofluorimeter equipped with a thermostatted cell holder and a magnetic stirrer. Excitation wavelength was 280 nm. Excitation and emission slits were set at 5 nm, and a cutoff filter of 290 nm was placed before the emission monochromator to minimize the contribution of the scattered light to the spectrum. Three spectra were taken for each sample after an incubation time of 15 min at 25°C. Spectra were corrected for the inner filter effect and the light scattered by the LUVs. For the correction of the inner filter effect, absorption spectra of all the samples (EqT-II with and without vesicles) were recorded in a Cary spectrophotometer, and we followed the procedure described by Lakowicz (1983). The light scattered by the LUVs was corrected by subtracting the corrected fluorescence signal of the vesicles

without EqT-II from the corrected spectrum of the protein in the presence of vesicles.

Surface pressure measurements

Surface pressure measurements were carried out with a μTrough S system from Kibron (Helsinki, Finland) at room temperature and under constant stirring. By using glass troughs with Teflon rims and stainless-steel magnetic bars we minimized the nonspecific adsorption of EqT-II to Teflon surfaces. The aqueous phase consisted of 450 μl of 10 mM Hepes, 200 mM NaCl, pH 7.5. The lipid, dissolved in chloroform/methanol (2:1), was gently spread over the surface, and the desired initial surface pressure was attained by changing the amount of lipid applied to the air-water interface. The protein was injected into the subphase with a Hamilton microsyringe through the lipid monolayer. Unless otherwise indicated, the final protein concentration in the Langmuir trough was 1.035 μM. The increment in surface pressure versus time was recorded, and the experimental data were fitted to the following equation:

$$y = y_0 + \frac{a \times x}{b + x}, \quad (3)$$

which corresponds to a rectangular hyperbola, where y stands for the increment in surface pressure, x is time, y_0 is the initial surface pressure, a is the maximum increase, and b is the time needed to reach 50% of the maximum increase. The fitting was carried out using the program Sigma Plot (SPSS, Science, Chicago, IL). The values obtained for y_0 are negative and permit us to estimate the true initial surface pressure after the perturbation caused by the injection of the protein into the subphase.

Interfacial hydropathy

To detect membrane-partitioning amino acid sequences in EqT-II, we plotted its average interfacial hydropathy. This approach makes use of a whole-residue scale that is based on the water-to-membrane interface transfer free energies for each amino acid (White and Wimley, 1996, 1999). In contrast to the classical indexes based on side-chain hydrophobicities alone, this scale takes into account side-chain and peptide bond hydrophobicity and compiles contributions arising from the bilayer effect. To infer the location within the membrane of partitioning sequences we also used a whole-residue hydrophobicity scale for partitioning into *n*-octanol. Plots based on the difference between the interfacial and octanol scales can in principle be used to distinguish sequences that prefer to insert deeply into the bilayer matrix from those that prefer associating with the interface (White and Wimley, 1999). Values above zero correspond to segments with higher tendency to remain associated with the membrane interface and values below zero are assigned to hydrophobic core-residing segments.

RESULTS

Effects of EqT-II on LUVs of different composition

When incubation of vesicles containing ANTS and DPX with EqT-II results in permeabilization there is an increase in the ANTS fluorescence. If, as a consequence of this interaction the vesicles aggregate, an increase in light scattering can be monitored by turbidity measurements. Table 1 summarizes the results obtained using LUVs of different lipid compositions.

TABLE 1 Effects of equinatoxin-II on LUVs of different compositions

Lipid	Leakage* (%)	Scattering† at 90°	Increase in size‡ (nm)
PC	3.8 ± 1.0	NO	7 ± 3
SM	15.6 ± 3.7	NO	3 ± 4
SM/PC (1:1)	76.1 ± 10.5	NO	5 ± 2
PC/DPPC (1:1)	1.6 ± 1.0	NO	ND
PC/PE/Cho (2:1:1)	0.8 ± 5.2	NO	11 ± 9
PC/Cho (7:3)§	41.4 ± 3.8	NO	ND

Lipid concentration was 0.1 mM and protein concentration was 1.3 μM (lipid-protein molar ratio = 77), except in QELS experiments, where both concentrations were doubled. Buffer was 10 mM Hepes, 200 mM NaCl, pH 7.5. The experiments were carried out at 25°C with constant stirring, except in the case of PC/Cho (7:3) where the temperature was 4°C.

*Leakage was determined 10 min after EqT-II addition. Results are the mean ± SD of three experiments.

†The right-angle scattering does not allow for quantitative analysis. The results indicate only whether there is a significant increase (>200%) of the signal in two separate experiments.

‡The increase in size with respect to the untreated vesicles are the mean ± SD of two experiments.

§Results obtained at 4°C.

We did not observe vesicle aggregation in any case. However, the toxin-induced permeabilization of the liposomes showed a marked dependence on lipid composition. Whereas PC LUVs are not sensible to the action of EqT-II, in LUVs made of PC/SM (1:1) 76% of the vesicle contents were released. This effect of SM has been known for many years, for this and other cytolysins from sea anemones (Bernheimer and Avigad, 1976; Turk and Maček, 1986; Tejuca et al., 1996). Surprisingly, under similar conditions, the release from vesicles containing only SM was very modest, as only 16% of the solutes leaked (Table 1). This observation contrasts with the results obtained in SUVs (Belmonte et al., 1993), where the release of calcein from vesicles made of SM was similar to that observed in vesicles made of PC/SM (1:1).

We used a mixture of egg-PC and DPPC (1:1) to determine whether the effect of SM could be mimicked by another lipid with a high phase transition temperature, but this was not the case, as is reflected in Table 1. Other lipid compositions, such as PC/PE/Cho (2:1:1), which is particularly well suited for the interaction with interface-seeking enzymes such as phospholipase C from *Bacillus cereus* (Basáñez et al., 1996), was also insensitive to EqT-II. It is possible, however, to find conditions in which leakage is observed in the absence of SM; PC LUVs containing 30% cholesterol can release up to 40% of their contents if we lower the temperature to 4°C.

Permeabilization of LUVs made of SM/PC (1:1)

In liposomes made of SM/PC (1:1), most of the vesicle contents are released without aggregation, and therefore, we

have chosen this lipid composition to further explore the EqT-II-induced permeabilization of LUVs. Fig. 1 represents the percentage of leakage and the halftime of the process as a function of protein concentration. An increase in protein concentration results in an increase in the percentage of leakage and a decrease in its $T_{1/2}$. Both parameters show a linear dependence with EqT-II concentration. This dependence is biphasic, and there is a point at which the slopes of the two lines change. This threshold value can be calculated as the intercept between the two regression lines that can be drawn from the experimental points and corresponds to an EqT-II concentration of 0.66 μM. Thus, at a lipid-protein molar ratio of 152, the incorporation of new protein molecules to the surface of the vesicles is hampered.

To rule out the possibility of a detergent effect as responsible for this leakage we have compared the EqT-II-induced leakage of ANTS from LUVs and from MLVs. If leakage were due to a detergent effect, the degree of leakage would be the same in LUVs and MLVs as it would depend only on the lipid-protein molar ratio, and not on the number of lamellae. This was not the case. In conditions where 55% of the vesicle contents were released in LUVs, the leakage in MLVs was only 14% (data not shown) and would correspond to the percentage of the total encapsulated volume that is surrounded by the outermost lipid bilayer.

EqT-II binding to PC/SM (1:1) LUVs

To determine the amount of EqT-II bound to the vesicles we added different amounts of protein to a fixed amount of liposomes. After an incubation period of 2 h, free and bound proteins were separated by ultrafiltration. Control experiments showed that the amount of protein adsorbed to the polysulfone filters was negligible (data not shown). The amount of free protein was estimated by its absorption at 280 nm, and the bound protein was calculated as the difference between total and free protein. Fig. 2 *A* represents the results obtained for three different lipid concentrations. The partition coefficients (K_x) ranged from 7.24×10^5 to 2.07×10^5, which represent a free energy of transfer from

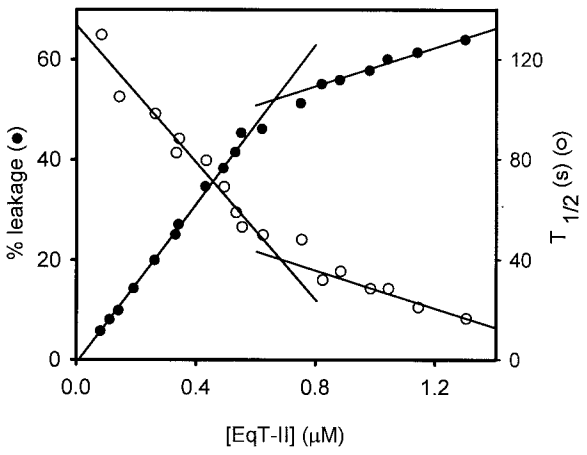

FIGURE 1 Equinatoxin-II-induced permeabilization of SM/PC (1:1) vesicles. To 1 ml of LUV (lipid concentration = 0.1 mM) containing ANTS/DPX, different amounts of equinatoxin-II were added. The percentage of leakage (●) was measured 15 min after protein addition and $T_{1/2}$ (○) is the time needed to achieve half of this leakage. Buffer was 10 mM Hepes, 200 mM NaCl, pH 7.5. The experiment was carried out at 25°C and with constant stirring. Each plot was fitted to two different regression lines.

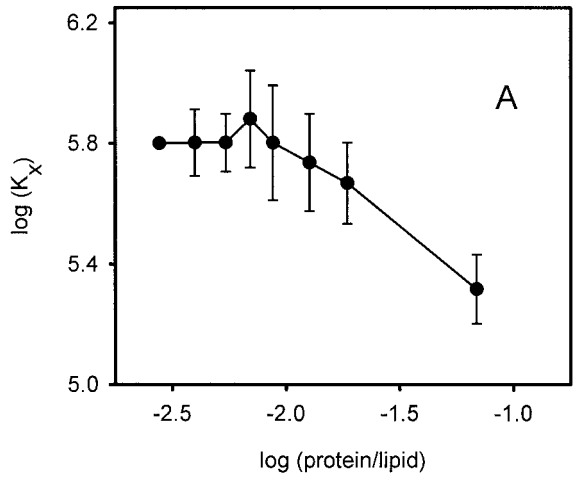

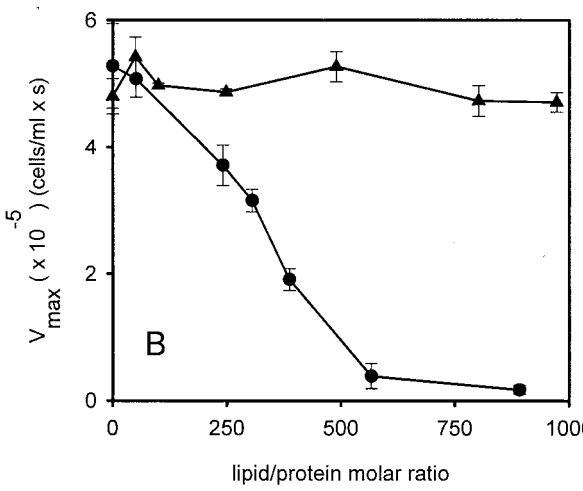

FIGURE 2 (*A*) Binding of EqT-II to SM/PC (1:1) vesicles. Different amounts of EqT-II were added to a fixed amount of vesicles. Free and bound protein was separated by ultrafiltration through polysulfone filters. The experiment was carried out in 10 mM Hepes, 200 mM NaCl, pH 7.5. Data correspond to the mean of three experiments at three different lipid concentrations (0.36, 0.53, and 0.66 mM, respectively). Bars indicate the standard deviation. (*B*) Reversibility of the binding. EqT-II at a fixed concentration of 0.7 μM was preincubated for 2 h at 25°C with LUVs made of PC (▲) or PC/SM (1:1) (●) at different molar ratios in 10 mM Hepes, 200 mM NaCl, pH 7.5 buffer. An aliquot of each mixture was added to an erythrocyte suspension containing 5.6×10^6 cells/ml, and the residual hemolytic activity was calculated from the changes in turbidity at 720 nm. Hemolysis was measured in 10 mM Hepes, 145 mM NaCl, 2 mM PEG 10,000, pH 7.5 buffer at 25°C with constant stirring. Data correspond to the mean of three experiments. Bars indicate standard deviation.

the aqueous to the lipid phase of −8.00 and −7.26 kcal mol^{-1}, respectively. It is important to observe that K_x remains fairly constant up to a protein-lipid ratio of 0.0069 (lipid-protein ratio = 145). Beyond this value, K_x decreases when the concentration of the protein increases, indicating that binding is anti-cooperative. This break point lies at the same lipid-protein ratio as that observed for the percentages and halftimes of leakage, thus suggesting that at this particular ratio the vesicles show evidence for protein saturation at the surface.

We used the same experimental approach to measure partitioning into PC vesicles and obtained a partition coefficient of 8.74×10^4 and a free energy of transfer from the aqueous to the lipid phase of −6.75 kcal mol^{-1}. Thus, although EqT-II does not produce any significant effect on LUVs made of PC, there is a significant fraction of the protein molecules that associates with the membrane surface.

To know whether the binding is reversible, we incubated EqT-II with LUVs for 2 h and then added an aliquot of this mixture to an erythrocyte suspension. As only unbound protein is able to produce hemolysis, if binding were reversible the degree of hemolysis would not be dependent on the lipid-protein molar ratio of the EqT-II-LUV incubation mixture. As Fig. 2 *B* shows, this seems to be the case for LUVs made of PC. However, for the case of LUVs made of PC/SM (1:1), as the lipid-protein molar ratio increases, the rate of hemolysis decreases and approaches zero when this ratio is 550 or higher, thus indicating that toxin binding to these vesicles must be irreversible.

Interfacial hydropathy

For EqT-II, the average interfacial hydrophobicity plot based on free energies of transfer from the membrane interface to water clearly identified one conspicuous area on the hydrophobic side above the zero midpoint line (Fig. 3). This positive peak is located between positions 101 and 121 and corresponds to the AVLFSVPYDYNWYSNWWNVRI sequence. The total free energy of partitioning of this sequence from water into the membrane, as estimated from the experimental scale determined by White and Wimley (1996) in POPC LUVs, is −5.98 kcal mol^{-1}. These observations would be consistent with the involvement of this fragment of the sequence in the initial transfer of EqT-II from the aqueous phase to the membrane interface. Within this fragment, the difference-scale plot (free energies of transfer from interface to octanol) shows that residues 104–117 give values above zero (Fig. 3, *inset*), suggesting that this region would have a marked tendency to lie on the bilayer interface rather than to penetrate deeper into the hydrophobic core.

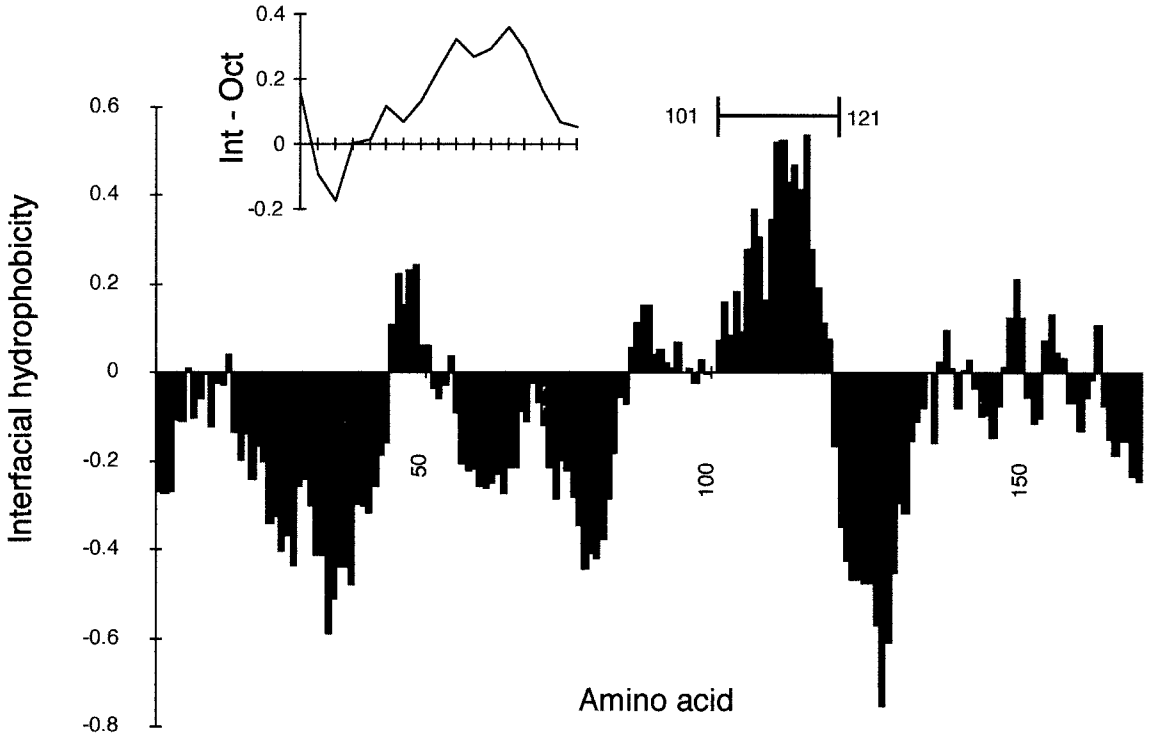

FIGURE 3 Hydropathy plot corresponding to the EqT-II sequence. The plot (mean values for a window of 11 amino acids) was elaborated using the Wimley-White interfacial hydrophobicity scale based on the free energy of transfer from the membrane-interface to the water phase. (*Inset*) Plot based on the difference of membrane-interface and *n*-octanol scales for the protein stretch spanning residues 101–117.

Infrared spectroscopy

The secondary structure of EqT-II in solution and in the presence of liposomes of PC or SM/PC (1:1) was studied by Fourier transform infrared spectroscopy (FTIR) at room temperature in deuterated medium. Whenever SM is present, an absorption band appears in the 1700–1600-cm^{-1} region, which is due to its amide group. Therefore, it was necessary to subtract the contribution of this group to analyze the behavior of the protein amide I band. To do this, we used the lipidic carbonyl absorption band (1750–1700 cm^{-1}) as reference and assumed that its elimination during the subtraction procedure cancels the contribution of the other lipidic absorption bands. In fact, when we obtained a flat baseline in that region, the vibration band of the lipidic methylene groups (2960–2940 cm^{-1}) also disappeared (data not shown), a result that confirms the reliability of this method.

Fig. 4 shows the amide I region of the FTIR spectrum of EqT-II in deuterated buffer and its decomposition and fitting. The amide I band is centered at 1641 cm^{-1} and presents a small shoulder around 1688 cm^{-1}. The fitting process gave rise to seven bands, centered at 1691, 1676, 1666, 1653, 1638, 1625, and 1613 cm^{-1}, respectively. The band centered at 1613 cm^{-1} corresponds to side chains, and therefore, it was not considered for further analysis. The bands centered at 1666, 1676, and 1691 cm^{-1} have been assigned to β-turns (Krimm and Bandekar, 1986). The band at 1676 cm^{-1} may also arise from a small contribution of the high-frequency vibration of the antiparallel β-strand (Byler and Susi, 1986). The band around 1655 cm^{-1} is characteristic of the α-helix (Arrondo et al., 1993). However, the assignation of the bands at 1638 and 1625 cm^{-1} is not so clear-cut. The band at 1625 cm^{-1} has been related to extended conformations that form intermolecular hydrogen bonds (Arrondo et al., 1988) or interact with other structural elements (Castresana et al., 1988). We do not think that this band is associated with protein aggregates (Naumann et al., 1993) because if this were the case, a band at 1685 cm^{-1} and a change in the shape of the amide I band would also be observed, and we have not detected these effects. Finally, the band at 1638 cm^{-1} could be assigned to a β-sheet (Krimm and Bandekar, 1986). However, contributions from other structural types might also be present because in H_2O a band at 1641 cm^{-1} appears, which does not correspond to a β structure (data not shown) and can be assigned to open loops (1644 cm^{-1}) (Fabian et al., 1992). Taken together, these results indicate that in solution, EqT-II consists of 44% β-sheet structures, 37% α-helix, and 17% turns.

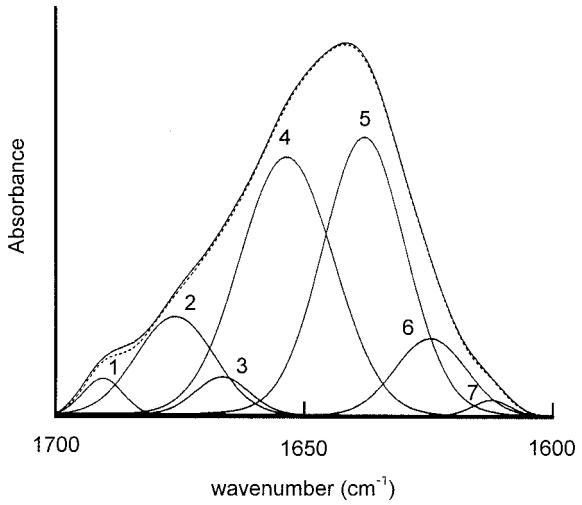

FIGURE 4 Fitting and deconvolution of the FTIR spectrum of EqT-II in deuterated buffer. The solid line corresponds to the amide I band of the FTIR spectrum of EqT-II and the dotted line is the resultant of the seven resolved bands, centered at 1691 (1), 1676 (2), 1666 (3), 1653 (4), 1638 (5), 1625 (6), and 1613 (7) cm^{-1}, respectively. Buffer was 10 mM Hepes, 200 mM NaCl, pD 7.9. The spectrum was recorded at 25°C.

Table 2 summarizes the results obtained after the decomposition and fitting of the FTIR spectra of EqT-II either in solution or in the presence of PC LUVs or SM/PC (1:1) LUVs. Only the results in D_2O are represented and are complementary to those obtained in water (data not shown). There are only little changes in secondary structure of EqT-II upon its interaction with PC vesicles. The most significant one is observed at the band centered at 1654 cm^{-1}, where the amount of α-helical structures decreases from 37% to 30%. Concomitantly, the amount of β-sheets increases from 44% to 47% and the percentage of β-turns increases from 17% to 21%. In contrast, EqT-II undergoes major conformational changes in the presence of LUVs of SM/PC (1:1). First, the band at 1666 cm^{-1} (corresponding to β-turns) disappears, although the overall contribution of this secondary structure element remains practically unchanged (16%, in comparison with 17% in solution). The most dramatic changes affect the α-helical structure, which is reduced from 37% in solution to 20% in the presence of vesicles, and the β-sheets, which increase from 44% in

TABLE 2 Decomposition and fitting of the amide I band of the infrared spectrum of EqT-II in solution and in the presence of LUVs of different composition

EqT-II		EqT-II + PC		EqT-II + SM/PC (1:1)	
Position (cm^{-1})	Area (%)	Position (cm^{-1})	Area (%)	Position (cm^{-1})	Area (%)
1691	2	1691	2	1692	1
1676	12	1676	14	1674	15
1666	3	1666	5	—	—
1653	37	1654	30	1657	20
1638	35	1639	34	1641	50
1625	9	1626	13	1626	13

Lipid concentration was 30 mM and protein concentration was 0.4 mM (lipid-protein molar ratio = 75). Buffer was 10 mM, Hepes, 200 mM NaCl, pD 7.9.

solution to 63% in the presence of LUVs. It is important to point out that the band that in solution is centered at 1638 cm^{-1} (which is assigned to β-sheet structure) is shifted to 1641 cm^{-1} and could also arise from contributions due to disordered structures (1643 cm^{-1}) or open loops (1644 cm^{-1}) (Cheín et al., 1999).

Intrinsic fluorescence

Changes in the intrinsic fluorescence of EqT-II can be associated with changes in its tertiary structure (Lakowicz, 1983). Fig. 5 represents the changes in fluorescence intensity (Fig. 5 *A*) and wavelength of maximum emission (Fig. 5 *B*) as a function of the lipid-protein ratio after incubation with LUVs made of PC or SM/PC (1:1). The addition of PC vesicles up to a lipid-protein molar ratio of 640 results in a 7% decrease in its fluorescence intensity without a shift in the wavelength of maximum emission. When the vesicles are made of SM/PC (1:1), there is a 24% fluorescence intensity increase and a blue shift in the wavelength of maximum emission from 336.5 nm in solution to 334 nm when the lipid-protein molar ratio is 600. These changes are consistent with the migration of the tryptophans to a more apolar environment like that provided by the membrane.

IR versus temperature

The thermal behavior of EqT-II as studied by FTIR provides us with more information about its differential interaction with LUVs of PC or SM/PC (1:1). In Fig. 6 we plot the changes in the bandwidth of the amide I region at half height as a function of the temperature, both in solution and in the presence of LUVs. This representation monitors the unfolding of the protein because its aggregation gives rise to the appearance of two bands at 1685 and 1620 cm^{-1} (data not shown) and, thus, to an increase of the width of the amide I band. In solution or in the presence of PC vesicles the thermal profile is sigmoidal and the inflection point is centered at 60°C. However, in the presence of SM/PC (1:1) LUVs, the behavior is totally different as the aggregation bands do not appear, and therefore the bandwidth of the amide I region remains constant. This means that either the protein is stable in the temperature range studied or that the interactions that are responsible for the cooperative thermal unfolding are already lost. This second possibility seems

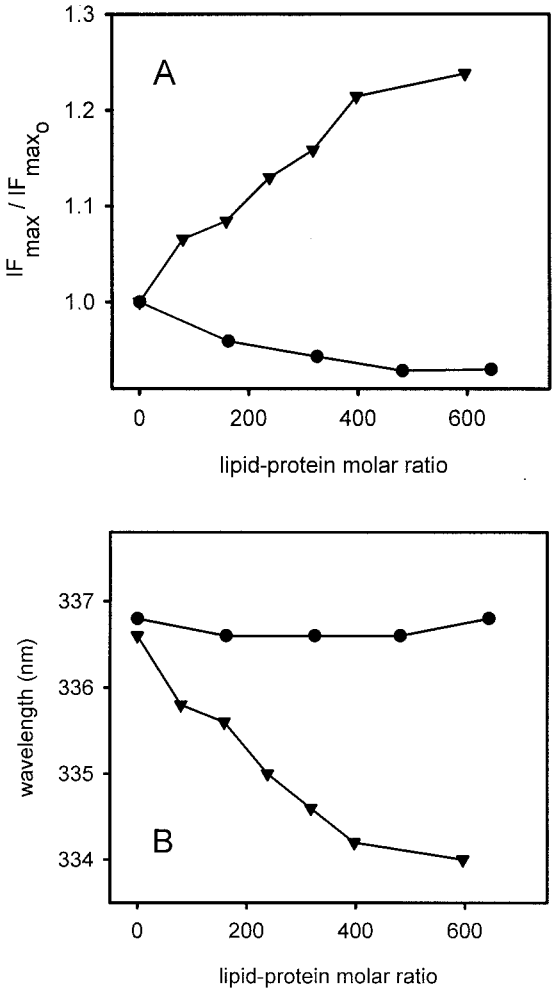

FIGURE 5 Intrinsic fluorescence of EqT-II in the presence of LUVs. (*A*) Changes in the relative fluorescence intensity of EqT-II in the presence of LUVs made of PC (●) or PC/SM (1:1) (▼). (*B*) Changes in the wavelength of maximum emission of EqT-II in the presence of LUVs made of PC (●) or PC/SM (1:1) (▼). Buffer was 10 mM Hepes, 200 mM NaCl, pH 7.5. The spectra were recorded at 25°C.

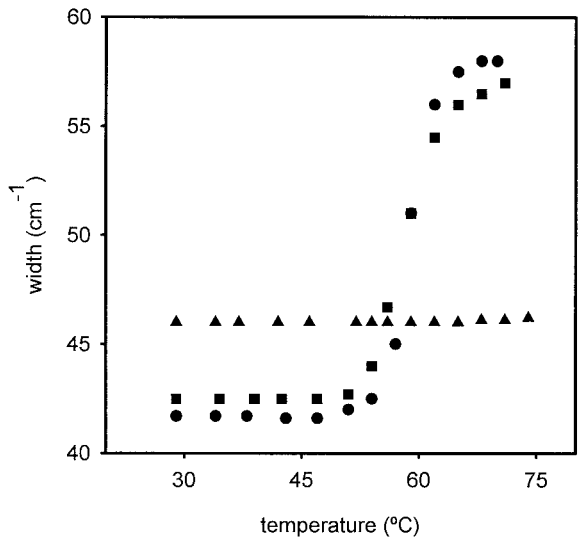

FIGURE 6 Effect of the temperature on the amide I bandwidth of EqT-II in solution (●), in the presence of LUVs made of PC (■) or in the presence of LUVs made of SM/PC (1:1) (▲). The deuterated buffer was 10 mM Hepes, 200 mM NaCl, pD 7.9. Protein concentration was 0.4 mM and the lipid-protein molar ratio was 75. Samples were incubated overnight at room temperature to allow for complete equilibration.

more likely in view of the changes in secondary and tertiary structure already described.

EqT-II insertion into phospholipid monolayers

We used lipid monolayers with different lipid compositions (PC, SM, and an equimolar mixture of PC and SM) to determine the critical pressure (π_c), i.e., the initial surface pressure (π_0) at which no $\Delta\pi$ is observed after injection of EqT-II into the subphase. This value can be estimated by plotting $\Delta\pi$ versus π_0 and extrapolating the data to the point at which $\Delta\pi = 0$. As shown in Fig. 7, $\Delta\pi$ decreased when π_0 increased, because the higher lipid packing prevents protein insertion. Linear fitting of the experimental results permitted us to estimate a critical pressure of 25.2 mN m^{-1} for PC, 25.85 mN m^{-1} for SM, and 32.7 mN m^{-1} for the equimolar mixture. The critical pressures for PC and SM are practically the same, probably because the structure of their polar headgroups is very similar and so is their contribution for the insertion of EqT-II. However, at any given π_0, the $\Delta\pi$ observed is higher for SM than for PC.

In the equimolar mixture of PC and SM the critical pressure was significantly higher than in the pure lipids, despite the fact that the polar headgroups of the lipids are the same. If we compare the results found in SM and in the SM/PC mixture, we again observe that at any given π_0, $\Delta\pi$ is higher in the mixture, although the overall dependence of $\Delta\pi$ versus π_0 (the slope of the regression lines) is the same,

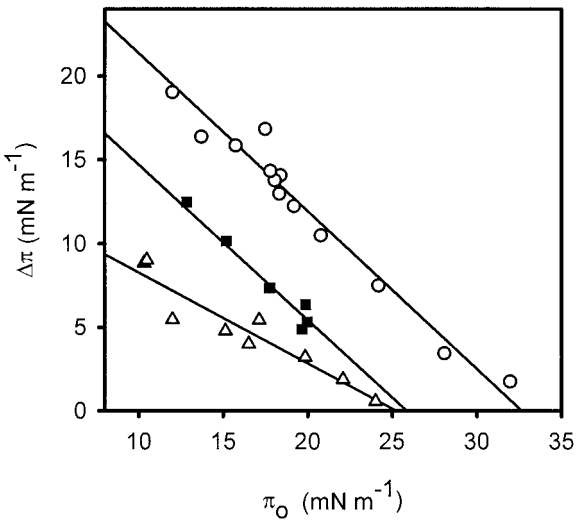

FIGURE 7 Effect of the initial surface pressure on the insertion of EqT-II into monolayers of different lipid composition. Lipid compositions were PC (△), SM (■), or PC/SM (1:1) (○). Experimental data were fitted to straight lines whose intercepts with the abscissa axis represent the critical pressure (π_c), i.e., the initial surface pressure at which the protein no longer inserts into the monolayer. Protein concentration was 0.97 μM and the buffer was 10 mM Hepes, 200 mM NaCl, pH 7.5. The experiments were carried out at room temperature with constant stirring.

−0.93 for SM and −0.94 for SM/PC (1:1), and is almost twice the value for PC (−0.54).

These results indicate that when conditions are favorable for insertion ($\pi_0 < \pi_c$), the affinity of EqT-II for SM is higher than for PC, and in the SM/PC equimolar mixture, the insertion is governed by the SM content.

DISCUSSION

SM favors the lytic action of EqT-II but is not essential

As in other cytolysins (Tejuca et al., 1996; De los Ríos et al., 1998), the presence of SM within the bilayer favors the release of encapsulated solutes by EqT-II (Table 1). However, in LUVs made of only SM, the percentage of leakage is only moderate (16%). This observation contrasts with the results obtained in SUVs (Belmonte et al., 1993; Maček et al., 1995), where the leakage of calcein and the changes in the intrinsic fluorescence of EqT-II are similar in SM and its equimolar mixture with PC. This different behavior observed for SUVs and LUVs has also been described for sticholysin I (Tejuca et al., 1996) and might be due to the fact that SUVs and LUVs represent two different model membranes. The radius of curvature in SUVs is so small that most of the lipids (up to 70%) tend to locate in the external monolayer (Szoka and Papahadjopoulus, 1980), thus establishing significant differences in the packing, thermotropic behavior, order, and lateral mobility of the lipids in comparison with LUVs or MLVs (New, 1990). All these effects also influence the interaction of the vesicles with proteins such as phospholipase C from *Bacillus cereus* (Basáñez et al., 1996), which is much more active in SUVs than in LUVs with the same lipid composition.

The absence of lytic activity in PC vesicles does not necessarily mean that there is no interaction. A partition coefficient of 8.74×10^4 and a free energy of transfer from the aqueous to the lipid phase of −6.75 kcal mol^{-1} have been measured, confirming that EqT-II associates with PC LUVs. Moreover, EqT-II inserts into PC monolayers provided that the initial surface pressure is lower than 26 mN m^{-1}. This result explains why we do not observe leakage in LUVs, because in this case, the estimated surface pressure of the lipids within the vesicles ranges between 30 and 35 mN m^{-1} (Brockman, 1999), clearly above its critical surface pressure. The critical pressures for SM and PC are the same (~26 mN m^{-1}), an observation that is not surprising, because both phospholipids have nearly identical polar headgroups. However, when the initial surface pressure is lower than this π_c, the toxin inserts to a greater extent into the pure SM monolayer, a result that might indicate that the hydrophobic component of the insertion is more important in SM monolayers. In these conditions, the packing of the lipids is not so rigid, and they may expose some regions that could be recognized by the toxin and, thus, explain the

preferential insertion into SM monolayers. A second possibility is that below π_c, the acyl chains of the commercially purchased brain SM (which show a certain degree of heterogeneity) may segregate laterally and form lipid domains that may favor the insertion, and this would account for the 16% leakage observed in LUVs made of SM. When the lipid monolayer is made of SM/PC (1:1), the critical pressure is 32.7 mN m^{-1}, and therefore, EqT-II is able to insert into LUVs with this lipid composition.

However, it is possible to find a variety of conditions under which EqT-II is active even in the absence of SM. This feature is common to other actinoporins. For instance, sticholysins from *Stichodactyla helianthus* increase the conductivity in planar lipid bilayers made of PC and cholesterol (Michaels, 1979), insert into DPPC monolayers (Doyle et al., 1989), are active in MLVs made of synthetic PC with various acyl lengths (Shin et al., 1979) and are able to permeabilize LUVs made of PC and cholesterol (De los Ríos et al., 1998). In the case of EqT-II, we have observed that addition of 20–30% cholesterol to PC results in 40% leakage from LUVs (Table 1) and monolayer insertion (data not shown). Therefore, the role of SM during the membrane insertion of EqT-II is not limited to act as a simple receptor, because other factors such as the radius of curvature of the vesicles and lipid-lipid interactions between SM and PC or between PC and cholesterol might be involved.

EqT-II binding to model membranes

In LUVs made of SM/PC (1:1), when the lipid-protein molar ratio is lower than 150, a given increment in the protein concentration gives rise to an increase in the percentage of leakage that is smaller than that observed at lipid-protein ratios above 150. This change also affects the halftime for this release and could be the result of a change in the amount of protein bound to the vesicles. Effectively, the partition coefficient of EqT-II between the lipidic and aqueous phases is fairly constant ($\log K_X = 5.82 \pm 0.1$) up to a lipid-protein molar ratio of 141, and below this value less protein partitions into the lipid phase; i.e., the binding is anti-cooperative. This anti-cooperativity must be a consequence of partial saturation of the surface of the vesicles by protein molecules. This result rules out the induction of a breach in the permeability barrier of the membrane by means of a detergent effect, as has been suggested with sticholysin (Shin et al., 1979). In identical experimental conditions, the leakage from LUVs is four times higher than from MLVs (unpublished results), confirming that the action of EqT-II is limited to the outermost lipid bilayer. The binding of the protein is essentially irreversible, because preincubation of EqT-II with PC/SM (1:1) liposomes results in a drastic decrease of its hemolytic activity (Fig. 2). The inhibitory effect of some membrane lipids on the hemolytic activity of EqT-II was described by Turk and Maček (1986), and they found the greatest inhibition with SM, although the lipids were organized in micelles rather than in vesicles. In contrast to what is observed with PC/SM (1:1) LUVs, the association of EqT-II with PC LUVs is reversible, as its hemolytic activity is retained after incubation with vesicles.

By using a hydropathy analysis based on the hydrophobicity-at-interface scale (White and Wimley, 1996; Pereira et al., 1997; Ruiz-Argüello et al., 1998), a conserved hydrophobic stretch of amino acids with high propensity to partition into membranes (Fig. 3) can be identified. The estimated total free energy of partitioning of this segment into POPC LUVs (White and Wimley, 1996) is −5.98 kcal mol^{-1}, very close to the experimental value (−6.67 kcal mol^{-1}) obtained with PC LUVs, thus confirming that this region might play a crucial role in the initial toxin-membrane interaction. By contrast, for SM-containing vesicles the free energy calculated for the partition of this region into the lipidic phase accounts for only 74% of the total experimentally calculated free energy of partitioning. This discrepancy might be originated from 1) the non-applicability of the same hydrophobicity-at-interface scale to estimate the energetics of the partitioning process in the binary system SM:PC or 2) the existence of other membrane-interacting regions in EqT-II, i.e., its N-terminal amphiphilic α-helix and/or the region containing amino acids Arg 144 and Ser 160 (Anderluh et al., 1999).

The pronounced hydrophobic-at-interface character of the region comprising amino acids 101–121 appears to be based on the unusual concentration of aromatic residues (one Phe, three Tyr, and three Trp) within such a short sequence. This is a feature that has been observed for other pore-forming toxins such as α-toxin from *Staphylococcus aureus* (Vécsey-Semjén et al., 1997; Raja et al., 1999) and perfringolysin-O (Sekino-Suzuki et al., 1996; Rossjohn et al., 1997). Extended analysis, including interface-octanol difference plots (White and Wimley, 1999; Nir and Nieva, 2000), demonstrates that the 104–117 sequence most probably localizes associated with the bilayer interface (Fig. 3 *inset*) rather than deeply inserted into the membrane hydrophobic core. This explains why the intrinsic fluorescence of EqT-II is not quenched by brominated lipids (Maček et al., 1995, and our unpublished results). This segment also coincides with one of the membrane-interacting regions delimited by Anderluh et al. (1999) in an elegant series of experiments with labeled cysteine mutants.

Differential interaction in response to lipid composition

In solution, equinatoxin II consists of 44% β-sheet structures, 37% α-helix, and 17% turns. EqT-II is, therefore, a β-rich protein as has been already observed by circular dichroism (CD) (Belmonte et al., 1994; Poklar et al., 1997). This feature is common to other actinoporins such as those of *Stichodactyla helianthus*. FTIR (Menestrina et al., 1999) and CD (De los Ríos, 1999) experiments show that the

amount of β-structure (β-sheet plus β-turns) in sticholysins accounts for more than 63% of the total secondary structure.

The thermal stability of EqT-II in solution or in the presence of LUVs made of PC are very similar. In both cases, the melting temperature is centered at 60°C (Fig. 6), a value that is very close to the denaturation temperature determined in solution by changes in the fluorescence of 1-anilinonaphthalene-8-sulfonic acid (59°C, data not shown) and similar to that obtained by differential scanning calorimetry (66°C in pure water, pH 5.5–6) (Poklar et al., 1997). The absence of a blue shift in the wavelength of maximum emission, the inability to produce the release of encapsulated solutes (Table 1), the conservation of its hemolytic activity (Fig. 2), and its thermal behavior (Fig. 6) suggest that EqT-II does not insert into PC vesicles. However, it must be somehow associated with the bilayer because 1) EqT-II is able to insert into PC monolayers provided that $\pi_0 < 26$ mN m^{-1}, 2) there are minor changes in secondary structure (Table 2) that might be responsible for the small decrease in its fluorescence intensity (Fig. 4), and 3) it contains an interface-seeking region comprising amino acids 104–117 (Fig. 3 *inset*).

The scenario is totally different in the presence of LUVs made of SM/PC (1:1). The insertion of EqT-II is manifested as a large increase in the surface pressure of lipid monolayers (Fig. 6), the release of solutes encapsulated in LUVs (Table 1), and an almost complete loss of hemolytic activity (Fig. 3). There are major changes in secondary structure: the β-structures increase to 79% (63% β-sheet and 16% β-turns), and the α-helical structures are reduced from 37% to 20%. These observations contrast with the CD results of Belmonte et al. (1994), who observed a large increase in α-helical structures upon interaction with SUVs. More recent CD results (Poklar et al., 1997) have shown that, effectively, there was an overestimation of the α-helical content of the protein. In the presence of LUVs made of SM/PC (1:1), EqT-II can be heated up to 75°C without observing any change in aggregation. This means that the protein must be localized in a stabilizing environment like that provided by the hydrophobic interior of the membrane. This is further corroborated by the changes in its intrinsic fluorescence (24% increase in intensity and a blue-shift of the λ_{max} of emission from 336.5 to 334 nm) that are typically associated with the transfer of the tryptophans to a less polar environment such as the hydrophobic core of a bilayer (Lakowicz, 1983). The fluorescence results described by Maček et al. (1995) with SUVs are qualitatively similar but quantitatively different, showing again that both model systems behave differently.

In conclusion, our results show that the interaction of EqT-II with model membranes is modulated by the lipid composition. In PC, the association is fully reversible, does not involve major conformational changes, and is mainly governed by the high affinity for membrane interfaces of the region comprising amino acids 101–120. The presence of SM within the membrane creates conditions for irreversible insertion and pore formation, processes that are associated with major conformational changes. The identification of those factors promoting the transition of EqT-II from a membrane-associated to a membrane-inserted state will be the subject of future investigations.

We thank Professor Paavo K. J. Kinnunen (University of Helsinki) for the use of the electrobalance and Langmuir trough. G. Anderluh is gratefully acknowledged for critical reading of the manuscript.

This work was supported by grants PI-1998–110 and UE-1998–43 from the Basque Government. J.M.M.C., I.E., and I.G.A. were recipients of predoctoral fellowships from the Basque Government.

REFERENCES

Anderluh, G., A. Barlič, Z. Podlesek, P. Maček, J. Pungerčar, F. Gubenšek, M. L. Zechinni, M. Dalla Serra, and G. Menestrina. 1999. Cysteine-scanning mutagenesis of an eukaryotic pore-forming toxin from sea anemone. Topology in lipid membranes. *Eur. J. Biochem.* 263:128–136.

Arrondo, J. L. R., A. Muga, J. Castresana, and F. M. Goñi. 1993. Quantitative studies of the structure of proteins in solution by Fourier-transform infrared spectroscopy. *Prog. Biophys. Mol. Biol.* 59:23–56.

Arrondo, J. L. R., N. M. Young, and H. H. Mantsch. 1988. The solution structure of concanavalin A probed by FT-IR spectroscopy. *Biochim. Biophys. Acta.* 952:261–268.

Bartlett, G. R. 1959. Phosphorus assay in column chromatography. *J. Biol. Chem.* 334:466–468.

Basáñez, G., J. L. Nieva, F. M. Goñi, and A. Alonso. 1996. Origin of the lag period in the phospholipase C cleavage of phospholipids in membranes. *Biochemistry.* 35:15183–15187.

Batista, U., K. Jezernik, P. Maček, and B. Sedmak. 1987. Morphological evidence of cytotoxic and cytolytic activity of equinatoxin II. *Period. Biol.* 89:347–348.

Belmonte, G., G. Menestrina, C. Pederzolli, I. Križeaj, F. Gubenšek, T. Turk and P. Maček. 1994. Primary and secondary structure of a pore-forming toxin from the sea anemone *Actinia equina* L., and its association with lipid vesicles. *Biochim. Biophys. Acta.*192:1197–204.

Belmonte, G., C. Pederzolli, P. Maček, and G. Menestrina. 1993. Pore formation by the sea anemone cytolysin equinatoxin II in red blood cells and model lipid membranes *J. Membr. Biol.* 131:11–22.

Bernheimer, A. W., and L. Avigad. 1976. Properties of a toxin from the sea anemone *Stoichactis helianthus*, including specific binding to sphingomyelin *Proc. Natl. Acad. Sci. U.S.A.* 73:467–471.

Brockman, H. 1999. Lipid monolayers: why use a half a membrane to characterize protein-membrane interactions? *Curr. Opin. Struct. Biol.* 9:438–443.

Bunc, M., G. Drevenšek, M. Budihna, and D. Šuput. 1999. Effects of equinatoxin II from *Actinia equina* (L.) on isolated rat heart: the role of direct cardiotoxic effects in equinatoxin II lethality. *Toxicon.* 37: 109–123.

Byler, D. M., and H. Susi. 1986. Examination of the secondary structure of proteins by deconvolved FT-IR spectra. *Biopolymers.* 25:469–487.

Castresana, J., A. Muga, and J. L. R. Arrondo. 1988. The structure of proteins in aqueous solutions: an assessment of triose phosphate isomerase structure by Fourier-transform infrared spectroscopy. *Biochem. Biophys. Res. Commun.* 152:69–75.

Cheín, R., I. Iloro, M. J. Marcos, E. Villar, V. L. Shnyrov, and J. L. R. Arrondo. 1999. Thermal and pH-induced conformational changes of a beta-sheet protein monitored by infrared spectroscopy. *Biochemistry.* 38:1525–1530.

De los Ríos, V. 1999. Caracterización y mecanismo de acción de la sticholisina II. Ph.D. thesis. Universidad Complutense de Madrid, Madrid.

De los Ríos, V., J. M. Mancheño, M. E. Lanio, M. Oñaderra, and J. G. Gavilanes. 1998. Mechanism of the leakage induced on lipid model membranes by the hemolytic protein sticholysin II from the sea anemone *Stichodactyla helianthus. Eur. J. Biochem.* 252:284–289.

Doyle, J. W., W. R. Kem, and F. A. Villalonga. 1989. Interfacial activity of an ion channel-generating protein cytolysin from the sea anemone *Stichodactyla helianthus. Toxicon.* 27:465–471.

Ellens, H., J. Bentz, and F. C. Szoka. 1985. H^+ and Ca^{2+}-induced fusion and destabilization of liposomes. *Biochemistry.* 24:3099–3106.

Fabian, H., D. Naumann, R. Misselwitz, O. Ristau, D. Gerlach, and H. Welfle. 1992. Secondary structure of streptokinase in aqueous solution: a Fourier transform infrared spectroscopic study. *Biochemistry.* 31: 6532–6538.

Giraldi, T., I. Ferlan, and D. Romeo. 1976. Antitumour activity of equinatoxin. *Chem. Biol. Interact.* 13:199–203.

Krimm, S., and J. Bandekar. 1986. Vibrational spectroscopy and conformation of peptides, polypeptides and proteins. *Adv. Protein Chem.* 38:181–364.

Lakowicz, J. R. 1983. Principles of Florescence Spectroscopy. Plenum Press, New York.

Maček, P., G. Belmonte, C. Pederzolli, and G. Menestrina. 1994. Mechanism of action of equinatoxin II, a cytolysin from the sea anemone *Actinia equina* L. belonging to the family of actinoporins. *Toxicology.* 87:205–227.

Maček, P., and D. Lebez. 1981. Kinetics of hemolysis induced by equinatoxin, a cytolytic toxin from the sea anemone *Actinia equina*. Effects of some ions and pH. *Toxicon.* 19:233–240.

Maček, P., and D. Lebez. 1988. Isolation and characterization of three lethal and hemolytic toxins from the sea anemone *Actinia equina* L. *Toxicon.* 26:441–451.

Maček, P., M. Zecchini, C. Pederzolli, M. Dalla Serra, and G. Menestrina. 1995. Intrinsic tryptophan fluorescence of equinatoxin II, a pore-forming polypeptide from the sea anemone *Actinia equina* L., monitors its interaction with lipid membranes. *Eur. J. Biochem.* 234:329–335.

Maček, P., M. Zecchini, K. Stanek, and G. Menestrina. 1997. Effect of membrane-partitioned n-alcohols and fatty acids on pore-forming activity of a sea anemone toxin. *Eur. Biophys. J.* 25:155–162.

Mayer, L. D., M. J. Hope, and P. R. Cullis. 1986. Vesicles of variable size produced by a rapid extrusion procedure *Biochim. Biophys. Acta.* 858: 161–168.

Menestrina, G., V. Cabiaux, and M. Tejuca. 1999. Secondary structure of sea anemone cytolysins in soluble and membrane bound form by infrared spectroscopy. *Biochem. Biophys. Res. Commun.* 254:174–180.

Michaels, D. W. 1979. Membrane damage by a toxin from sea anemone *Stoichactis helianthus. Biochim. Biophys. Acta.* 555:67–78.

Naumann, D., C. Schultz, U. Görne-Tschelnokow, and F. Hucho. 1993. Secondary structure and temperature behaviour of the acetylcholine receptor by Fourier transform infrared spectroscopy. *Biochemistry.* 32: 3162–3168.

New, R. R. C. 1990. Liposomes, A Practical Approach. IRL Press, Oxford.

Nir, S., and J. L. Nieva. 2000. Interaction of peptides with liposomes: pore formation and fusion. *Prog. Lipid Res.* 39:181–206.

Norton, R. S., P. Maček, G. E. Reid, and R. J. Simpson. 1992. Relationship between the cytolysins tenebrosin C from *Actinia tenebrosa* and equinatoxin II from *Actinia equina. Toxicon.* 30:13–23.

Pereira, F. B., F. M. Goñi, A. Muga, and J. L. Nieva. 1997. Permeabilization and fusion of uncharged lipid vesicles induced by the HIV-1 fusion peptide adopting extended conformation: dose and sequence effects. *Biophys. J.* 73:1977–1986.

Poklar, N., J. Fritz, P. Maček, G. Vesnaver, and T. V. Chalikian. 1999. Interaction of the pore-forming protein equinatoxin II with model lipid membranes: a calorimetric and spectroscopic study. *Biochemistry.* 38: 14999–15008.

Poklar, N., J. Lah, M. Salobir, P. Maček, and G. Vesnaver. 1997. pH and temperature-induced molten globule-like denatured states of equinatoxin II: a study by UV-melting, DSC, far- and near-UV CD spectroscopy and ANS fluorescence. *Biochemistry.* 36:14345–14352.

Raja, S. M., S. S. Rawat, A. Chattopadhyay, and A. K. Lala. 1999. Localization and environment of tryptophans in soluble and membrane-bound states of a pore-forming toxin from *Staphylococcus aureus. Biphys. J.* 76:1469–1479.

Rossjohn, J., S. C. Feil, W. J. McKinstry, R. K. Tweten, and M. W. Parker. 1997. Structure of a cholesterol-binding, thiol-activated cytolysin and a model of its membrane form. *Cell.* 89:685–692.

Ruiz-Argüello, M. B., F. M. Goñi, F. B. Pereira, and J. L. Nieva. 1998. Phosphatidylinositol-dependent membrane fusion induced by a putative fusogenic sequence of Ebola virus. *J. Virol.* 72:1775–1781.

Sekino-Suzuki, N., M. Nakamura, K. I. Mitsui, and Y. Ohno-Iwashita. 1996. Contribution of individual tryptophan residues to the structure and activity of theta-toxin (perfringolysin O), a cholesterol-binding cytolysin. *Eur. J. Biochem.* 241:941–947.

Shin, M. L., D. W. Michaels, and M. M. Mayer. 1979. Membrane damage by a toxin from the sea anemone *Soichactis helianthus*. II. Effect of membrane lipid composition in a liposome system. *Biochim. Biophys. Acta.* 555:79–88.

Szoka, F. C., and D. Papahadjopoulus. 1980. Comparative properties and methods of preparation of lipid vesicles (liposomes). *Annu. Rev. Biophys. Bioenerg.* 9:467–508.

Tejuca, M., M. Dalla Serra, M. Ferreras, M. E. Lanio, and G. Menestrina. 1996. Mechanism of membrane permeabilization by sticholysin I, a cytolysin isolated from the venom of the sea anemone *Stichodactyla helianthus. Biochemistry.* 35:14947–14957.

Teng, C. M., C. Y. Lee, and I. Ferlan. 1988. Platelet aggregation induced by equinatoxin. *Thromb. Res.* 52:401–411.

Turk, T., and P. Maček. 1986. Effect of different membrane lipids on the hemolytic activity of equinatoxin II from *Actinia equina. Period. Biol.* 88:216–217.

Vécsey-Semjén, B., C. Lesieur, R. Möllby, and F. G. van der Goot. 1997. Conformational changes due to membrane binding and channel formation by staphylococcal α-toxin. *J. Biol. Chem.* 272:5709–5717.

White, S. H., and W. C. Wimley. 1996. Experimentally determined hydrophobicity scale for proteins at membrane interfaces. *Nat. Struct. Biol.* 3:842–848.

White, S. H., and W. C. Wimley. 1999. Membrane protein folding and stability: physical principles. *Annu. Rev. Biophys. Biomol. Struct.* 28: 319–365.

White, S. H., W. C. Wimley, A. S. Ladokhin, and F. Hristova. 1998. Protein folding in membranes: determining energetics of peptide-bilayer interactions. *Methods Enzymol.* 295:62–87.

Zorec, R., M. Tester, P. Maček, and W. T. Mason. 1990. Cytotoxicity of equinatoxin II from the sea anemone *Actinia equina* involves ion channel formation and an increase in intracellular calcium activity. *J. Membr. Biol.* 118:243–249.